

3  
4 **Mitochondrial respiratory states and rates**

5  
6 Gnaiger Erich et al (MitoEAGLE Task Group)\*

7  
8 Corresponding author: Erich Gnaiger

9 *Chair COST Action CA15203 MitoEAGLE – <http://www.mitoeagle.org>*

10 *Department of Visceral, Transplant and Thoracic Surgery, D. Swarovski Research Laboratory,*

11 *Medical University of Innsbruck, Innrain 66/4, A-6020 Innsbruck, Austria*

12 *Email: mitoeagle@i-med.ac.at; Tel: +43 512 566796, Fax: +43 512 566796 20*

13  
14 Running title: Mitochondrial states and rates

15  
16 **As the knowledge base and importance of mitochondrial physiology to evolution, health, and**  
17 **disease expands, the necessity for harmonizing the terminology concerning mitochondrial**  
18 **respiratory states and rates has become increasingly apparent. The chemiosmotic theory**  
19 **establishes the mechanism of energy transformation during the process of oxidative**  
20 **phosphorylation (OXPHOS), providing the theoretical foundation of mitochondrial physiology**  
21 **and bioenergetics. We follow guidelines of the International Union of Pure and Applied Chemistry**  
22 **(IUPAC) on terminology, extended by considerations of mitochondrial respiratory control,**  
23 **metabolic flows and fluxes. The OXPHOS-capacity is respiration measured at kinetically-**  
24 **saturating concentrations of adenosine diphosphate, inorganic phosphate, and oxidizable**  
25 **substrates. The oxidative electron transfer-capacity reveals a possible limitation of OXPHOS-**  
26 **capacity mediated by the phosphorylation-pathway and is measured as noncoupled respiration at**  
27 **optimum concentrations of external uncouplers. Intrinsically uncoupled oxygen consumption**  
28 **compensates for ion leaks, particularly the proton leak. This LEAK-respiration is studied in the**  
29 **absence of ADP or by inhibition of the phosphorylation-pathway. Uniform standards for**  
30 **evaluation of respiratory states and rates will ultimately contribute to reproducibility between**  
31 **laboratories and thus support the development of databases of mitochondrial respiratory function**  
32 **in species, tissues, and cell types. Clarity of concept and consistency of nomenclature facilitate**  
33 **effective transdisciplinary communication, education, and ultimately further discovery.**

34  
35 *Keywords:* Mitochondrial respiratory control, coupling control; mitochondrial preparations;  
36 protonmotive force: *pmF*; uncoupling; oxidative phosphorylation: OXPHOS; electron transfer: ET;  
37 electron transfer system: ETS; proton leak, ion leak and slip compensatory state: LEAK; residual oxygen  
38 consumption: ROX; State 2; State 3; State 4; normalization; flow; flux; oxygen: O<sub>2</sub>; nicotinamide  
39 adenine dinucleotide: NADH

40  
41 **Harmonization of nomenclature**

42  
43 Mitochondria are essential cellular, membrane-enclosed organelles that perform a wide range of  
44 functions critical for cell viability. Their best-known function is to synthesize adenosine triphosphate  
45 (ATP) *via* oxidative phosphorylation (OXPHOS), however, they also have essential functions related to  
46 cellular metabolism and cell-signalling. This importance has led to an increasing body of research  
47 devoted to better understanding mitochondrial respiratory function. However, the dissemination of  
48 fundamental knowledge and implementation of novel discoveries require communication with a  
49 commonly understood terminology. Reproducibility of experimental procedures also depends on  
50 strictly-defined conditions and harmonization of shared research protocols. Unfortunately, a consensus  
51 on nomenclature and conceptual coherence is currently missing in the expanding field of mitochondrial  
52 physiology and bioenergetics. The use of vague, ambiguous, or inconsistent terminology likely  
53 contributes to confusion, miscommunication, and the conversion of valuable signals to wasteful noise.

54 Thus, complementary to quality control a conceptual framework is required to standardise and  
55 harmonise terminology and methodology.

56 To fill this communication gap, this perspective aims to harmonize nomenclature and addresses  
57 the terminology on coupling states and fluxes through metabolic pathways of aerobic energy  
58 transformation in mitochondrial (mt) preparations. In an attempt to establish a transdisciplinary  
59 nomenclature, we strive to incorporate a concept-driven terminology of bioenergetics with explicit,  
60 easily recognizable terms and symbols that define mitochondrial respiratory states and rates. The  
61 consistent use of terms and symbols will facilitate transdisciplinary communication for quantitative  
62 modelling and data repositories on bioenergetics and mitochondrial physiology<sup>1-3</sup>.

## 64 Coupling in mitochondrial respiration

65  
66 **Respiration and fermentation.** Aerobic respiration is the O<sub>2</sub> flux in (1) OXPHOS with catabolic  
67 reactions leading to O<sub>2</sub> consumption coupled to phosphorylation of ADP to ATP, plus (2) O<sub>2</sub> consuming  
68 reactions apart from OXPHOS. Coupling of electron transfer (ET) to ADP→ATP conversion is mediated  
69 by vectorial translocation of protons across the mitochondrial inner membrane (mtIM). Proton pumps  
70 generate, or utilize the electrochemical protonmotive force, *pmF* (Fig. 1). The *pmF* is the sum of two  
71 partial forces, the electric force (electric potential difference across the mtIM) and chemical force  
72 (proton chemical potential difference, related to ΔpH)<sup>4,5</sup>. Cell respiration is thus distinguished from  
73 fermentation: (1) Compartmental coupling in vectorial OXPHOS contrasts to substrate-level  
74 phosphorylation in fermentation without requirement for O<sub>2</sub><sup>4,5</sup>. (2) Redox balance is maintained in  
75 aerobic respiration by O<sub>2</sub> as the electron acceptor supplied externally, whereas fermentation is  
76 characterized by internal electron acceptors formed in intermediary metabolism (Fig. 1a).

77  
78 **Respiratory states and respiratory capacity.** Cell membranes include organellar membranes and the  
79 plasma membrane, which separates the intracellular milieu from the extracellular environment (Fig. 1a).  
80 The plasma membrane consists of a lipid bilayer with embedded proteins and attached organic  
81 molecules that collectively control the selective permeability of ions, organic molecules and particles,  
82 limiting the passage of many water-soluble mitochondrial substrates and inorganic ions. Such limitations  
83 are overcome in mitochondrial preparations: plasma membranes are removed or selectively  
84 permeabilized, while mitochondrial structural and functional integrity is maintained<sup>6</sup>. In mt-  
85 preparations, extramitochondrial concentrations of oxidizable ‘fuel’ substrates, ADP, ATP, inorganic  
86 phosphate (P<sub>i</sub>), and cations including H<sup>+</sup> can be controlled to determine mitochondrial respiratory  
87 function under a set of conditions defined as coupling control states (Tab. 1). In substrate-uncoupler-  
88 inhibitor titration protocols, substrate combinations and specific inhibitors of ET-pathway enzymes are  
89 used to obtain defined pathway control states<sup>7,8</sup> (Fig. 1b). Pathway and coupling control states are  
90 complementary, since mt-preparations depend on (1) an exogenous supply of pathway-specific fuel  
91 substrates and O<sub>2</sub>, and (2) exogenous control of phosphorylation<sup>9</sup>.

92 Reference respiratory states are established with kinetically-saturating substrate concentrations  
93 for analysis of mitochondrial respiratory capacities. These delineate — comparable to channel capacity  
94 in information theory<sup>10</sup> — the upper limit of O<sub>2</sub> consumption rates. Intracellular conditions in living  
95 cells may deviate from these experimental states. Further information is obtained in kinetic studies of  
96 flux as a function of fuel substrate concentration, [ADP], or [O<sub>2</sub>] in the range between kinetically-  
97 saturating concentrations and anoxia<sup>11</sup>.

98  
99 **Phosphorylation.** The term phosphorylation is used generally in many contexts, *e.g.*, protein  
100 phosphorylation. Phosphorylation in the context of OXPHOS is defined as phosphorylation of ADP by  
101 P<sub>i</sub> to form ATP, coupled to oxidative electron transfer (Fig. 1c,d). The ET- and phosphorylation-  
102 pathways comprise coupled components of the OXPHOS-system. P/O is the ratio of P<sub>i</sub> to atomic oxygen  
103 consumed<sup>9</sup>. The symbol, P<sub>»</sub>, is introduced here as more discriminating and specific than P (Fig. 1c). The  
104 symbol P<sub>»</sub> indicates the endergonic (uphill) direction ADP→ATP, and likewise P<sub>«</sub> the corresponding  
105 exergonic (downhill) hydrolysis ATP→ADP (Fig. 2). J<sub>P<sub>»</sub></sub> and J<sub>P<sub>«</sub></sub> are the corresponding fluxes of ADP  
106 phosphorylation and ATP hydrolysis, respectively. P<sub>»</sub> refers to phosphorylation driven by proton  
107 translocation (Fig. 1d)<sup>12</sup>, but may also involve substrate-level phosphorylation in the mitochondrial  
108 matrix (succinyl-CoA ligase, monofunctional C1-tetrahydrofolate synthase), cytosol (phosphoglycerate  
109 kinase and pyruvate kinase), or both (phosphoenolpyruvate carboxykinase isoforms 1 and 2). Kinase

110 cycles are involved in intracellular energy transfer and signal transduction for regulation of energy  
 111 flux<sup>13</sup>.

112

## 113 **Respiratory coupling control states: concept and nomenclature**

114

115 **Concept-driven terminology.** Respiratory control refers to the ability of mitochondria to adjust O<sub>2</sub> flux  
 116 in response to external control signals by engaging various mechanisms of control and regulation<sup>14</sup>.  
 117 Respiratory control is monitored in mt-preparations under conditions defined as ‘respiratory states’,  
 118 preferentially under near-physiological conditions of temperature, pH, and medium ionic composition.  
 119 When phosphorylation of ADP to ATP is stimulated or depressed, an increase or decrease is observed  
 120 in electron transfer. This is measured as O<sub>2</sub> flux in respiratory coupling states of intact mitochondria  
 121 (‘controlled states’ in the classical terminology of bioenergetics). Alternatively, the coupling of electron  
 122 transfer with phosphorylation is diminished by uncouplers, which eliminates control by P<sub>»</sub> and may  
 123 increase respiratory rate (noncoupled or ‘uncontrolled state’; **Tab. 1**).

124 Coupling efficiency is diminished by both intrinsic and extrinsic uncoupling. Uncoupling of  
 125 mitochondrial respiration is a general term comprising diverse mechanisms. Differences of terms —  
 126 uncoupled *vs.* noncoupled — are easily overlooked, although they relate to different meanings of  
 127 uncoupling (**Tab. 2**).

128 To extend the classical nomenclature on mitochondrial states (State 1 to 5)<sup>15</sup> by a concept-driven  
 129 terminology that explicitly incorporates information on the meaning of respiratory states, the  
 130 terminology must be general, and not restricted to any particular experimental protocol or type of  
 131 mitochondrial preparation<sup>16</sup>. Standard respiratory coupling states are obtained while maintaining a  
 132 defined ET-pathway state with constant fuel substrates and inhibitors of specific branches of the ET-  
 133 pathway. The focus of concept-driven nomenclature is primarily the theoretical *why*, along with  
 134 clarification of the experimental *how*<sup>17</sup>.

135 In the three coupling states — LEAK, OXPHOS, and ET — the corresponding respiratory rates  
 136 are abbreviated as *L*, *P*, and *E*, respectively (**Fig. 2a**). The *pmF* is *maximum* in the LEAK-state of coupled  
 137 mitochondria, driven by LEAK-respiration at a minimum back-flux of cations to the matrix  
 138 compartment, *high* in the OXPHOS-state when it drives phosphorylation, and *low* in the ET-state when  
 139 uncouplers short-circuit the proton cycle (**Tab. 1**).

140

141 **LEAK-state - Fig. 2b.** The LEAK-state is the state of mitochondrial respiration when O<sub>2</sub> flux mainly  
 142 compensates for ion leaks in the absence of ATP synthesis at kinetically-saturating concentrations of O<sub>2</sub>  
 143 and fuel substrates. Stimulation of phosphorylation is prevented by (1) absence of ADP and ATP; (2)  
 144 maximum ATP/ADP ratio (State 4); or (3) inhibition of the phosphorylation-pathway with inhibitors of  
 145 F<sub>1</sub>F<sub>0</sub>-ATPase (oligomycin; Omy) or adenine nucleotide translocase (carboxyatractyloside; **Tab. 1**). The  
 146 chelator EGTA is added to mt-respiration media to bind free Ca<sup>2+</sup>, thus limiting cation cycling. LEAK-  
 147 respiration is the intrinsically uncoupled O<sub>2</sub> consumption without addition of uncouplers. The LEAK-  
 148 rate is a function of respiratory state, hence it depends on (1) the barrier function of the mtIM  
 149 (‘leakiness’), (2) the electrochemical potential differences and concentration differences across the  
 150 mtIM, and (3) the H<sup>+</sup>/O<sub>2</sub> ratio of the ET-pathway (**Fig. 1b**).

151 State 4 is a LEAK-state after depletion of ADP<sup>15</sup>. O<sub>2</sub> flux in State 4 overestimates LEAK-  
 152 respiration if ATP hydrolysis activity recycles ATP to ADP,  $J_{P_{«}}$ , which stimulates respiration coupled  
 153 to phosphorylation,  $J_{P_{»}} > 0$ . Inhibition of the phosphorylation-pathway by oligomycin ensures that  $J_{P_{»}} =$   
 154 0 (State 4o; **Tab. 1**).

155

156 **OXPHOS-state - Fig. 2c.** At any given ET-pathway state, the OXPHOS-state establishes conditions to  
 157 measure OXPHOS-capacity as a reference, at kinetically-saturating concentrations of O<sub>2</sub>, as well as fuel  
 158 and phosphorylation substrates. Respiratory OXPHOS-capacities, *P*, are related to ADP-  
 159 phosphorylation capacities by the ATP yield per O<sub>2</sub> (**Fig. 1c**).

160 The OXPHOS-state is compared with State 3, which is the state stimulated by addition of fuel  
 161 substrates while the ADP concentration in the preceding State 2 (see below) is still ‘high’ and supports  
 162 coupled energy transformation in isolated mitochondria in a closed respirometric chamber<sup>15</sup>. Repeated  
 163 ADP titrations re-establish State 3. Starting at experimental O<sub>2</sub> concentrations of air-saturation (193 or  
 164 238 μM O<sub>2</sub> at 37 °C or 25 °C and sea level at 1 atm or 101.32 kPa, and an O<sub>2</sub> solubility of respiration  
 165 medium at 0.92 times that of pure water)<sup>18</sup>, the ADP concentrations must be low enough (typically 100

166 to 300  $\mu\text{M}$ ) to allow phosphorylation to ATP without  $\text{O}_2$  depletion during the transition to State 4. In  
 167 contrast, kinetically-saturating ADP concentrations are usually 10-fold higher than 'high ADP' (e.g., 2.5  
 168 mM) supporting OXPHOS capacity in isolated mitochondria<sup>11</sup>.

169  
 170 **Electron transfer-state - Fig. 2d.** The ET-state is defined as the *noncoupled* state with kinetically-  
 171 saturating concentrations of  $\text{O}_2$  and respiratory substrate, at the optimum concentration of exogenous  
 172 uncoupler for maximum  $\text{O}_2$  flux (ET-capacity). Uncouplers are weak lipid-soluble acids that function  
 173 as protonophores. These disrupt the barrier function of the mtIM and thus short-circuit the protonmotive  
 174 system, functioning like a clutch in a mechanical device. As a consequence of the nearly collapsed *pmF*,  
 175 the driving force is insufficient for phosphorylation and  $J_{P_s} = 0$ . The most frequently used uncouplers  
 176 are carbonyl cyanide *m*-chloro phenyl hydrazone (CCCP), carbonyl cyanide *p*-  
 177 trifluoromethoxyphenylhydrazone (FCCP), or dinitrophenol (DNP). Stepwise titration of uncouplers  
 178 stimulates respiration up to or above the level of  $\text{O}_2$  consumption rates in the OXPHOS-state; respiration  
 179 is inhibited, however, above optimum uncoupler concentrations<sup>5</sup>.

180 The abbreviation State 3u is occasionally used to indicate the state of respiration after titration of  
 181 an uncoupler, without sufficient emphasis on the fundamental difference between OXPHOS-capacity  
 182 (*well-coupled* with an endogenous uncoupled component) and ET-capacity (*noncoupled*; Fig. 2a).

183  
 184 **ROX-state versus anoxia.** The state of residual  $\text{O}_2$  consumption, ROX, is not a coupling state. The rate  
 185 of residual oxygen consumption, *Rox*, is defined as  $\text{O}_2$  consumption due to oxidative reactions measured  
 186 after inhibition of ET with antimycin A alone, or in combination with rotenone and malonic acid.  
 187 Cyanide and azide not only inhibit CIV, but also catalase and several peroxidases, whereas alternative  
 188 quinol oxidase is not inhibited (Fig. 1b). *Rox* represents a baseline to correct respiration: *Rox*-corrected  
 189 *L*, *P* and *E* are not only lower than total fluxes, but also change the flux control ratios *L/P* and *L/E*. *Rox*  
 190 is not necessarily equivalent to non-mitochondrial respiration. This is important when considering  $\text{O}_2$ -  
 191 consuming reactions in mitochondria that are not related to ET — such as  $\text{O}_2$  consumption in reactions  
 192 catalyzed by monoamine oxidases, monooxygenases (cytochrome P450 monooxygenases),  
 193 dioxygenases (trimethyllysine dioxygenase), and several hydroxylases.

194 In the nomenclature of Chance and Williams, State 2 is induced by titration of ADP before  
 195 addition of oxidizable substrates<sup>15,19</sup>. ADP stimulates respiration transiently on the basis of endogenous  
 196 fuel substrates resulting in phosphorylation of a small portion of the added ADP. State 2 is then a ROX  
 197 state at minimum respiratory activity after exhaustion of endogenous fuel substrates. State 5 '*may be*  
 198 *obtained by antimycin A treatment or by anaerobiosis*'<sup>15</sup>. These definitions give State 5 two different  
 199 meanings: ROX or anoxia.

200 Anoxia is induced after exhaustion of  $\text{O}_2$  in a closed respirometric chamber. Diffusion of  $\text{O}_2$  from  
 201 the surroundings into the aqueous solution is a confounding factor potentially preventing complete  
 202 anoxia<sup>11</sup>.

203

## 204 Rates and SI units

205

206 The term *rate* is not adequately defined to be useful for reporting data. A rate can be an extensive  
 207 quantity<sup>1</sup>, termed *flow*, *I*, when expressed (1) per chamber (instrumental system), or (2) per countable  
 208 object (number of cells, organisms,  $N_x$ ). Alternatively, a rate is a size-specific quantity<sup>2</sup>, termed *flux*, *J*,  
 209 when expressed (3) per volume of the chamber, *V*, or (4) per volume of the sample,  $V_x$ , or mass,  $m_x$  (Fig.  
 210 3).

211 Different units are used to report the  $\text{O}_2$  consumption rate, OCR. SI units provide a common  
 212 reference with appropriately chosen SI prefixes<sup>1</sup>. Although volume is expressed as  $\text{m}^3$  using the SI base  
 213 unit, the liter [ $\text{dm}^3$ ] is a conventional unit of volume for concentration and is used for most solution  
 214 kinetics. Constants for conversion to SI units are summarized in Tab. 3a.

215

## 216 Normalization of rate per system

217

218 **Flow: per chamber.** The instrumental system (chamber) is part of the measurement instrument,  
 219 separated from the environment by a closed or open system boundary. Analyses are restricted to intra-

220 experimental comparison of relative differences, when reporting  $O_2$  flows per respiratory chamber,  $I_{O_2}$   
 221  $[\text{mol}\cdot\text{s}^{-1}]$  (Fig. 3).

222

223 **Flux: per chamber volume.** System volume-specific  $O_2$  flux,  $J_{V,O_2}$  (per liquid  $V$  of the instrumental  
 224 chamber  $[\text{L}=\text{dm}^3]$ ), is of methodological interest in relation to the instrumental limit of detection.  $J_{V,O_2}$   
 225 increases in proportion to sample concentration in the chamber.  $J_{V,O_2}$  should be independent of the  
 226 chamber volume at constant sample concentration. There are practical limitations to increasing the  
 227 sample concentration in the chamber, when one is concerned about crowding effects and instrumental  
 228 time resolution.

229

## 230 Normalization of rate per sample

231

232 **Flow: per object.** A sample,  $X$ , may contain countable, non-divisible ('in-dividual') objects with a  
 233 variable number of objects,  $N_X$ . The number concentration of  $X$  is  $C_{NX}$ . Accordingly, the experimental  
 234 number concentration of cells,  $C_{Nce} = N_{ce}\cdot V^{-1}$ , is the number of cells,  $N_{ce}$  [x], per chamber volume,  $V$  [L].  
 235 Volume-specific  $O_2$  flux,  $J_{V,O_2}$   $[\text{mol}\cdot\text{s}^{-1}\cdot\text{L}^{-1}]$  divided by  $C_{NX}$   $[\text{x}\cdot\text{L}^{-1}]$  yields the oxygen flow per cell,  $I_{O_2/Nce}$   
 236  $[\text{mol}\cdot\text{s}^{-1}\cdot\text{x}^{-1}]$ . Here we write the dimensionless non-SI unit [x] explicitly, to distinguish the unit for flow  
 237 per object,  $I_{O_2/NX}$   $[\text{mol}\cdot\text{s}^{-1}\cdot\text{x}^{-1}]$ , from flow per chamber,  $I_{O_2}$   $[\text{mol}\cdot\text{s}^{-1}]$ . For convenience,  $O_2$  flow is  
 238 expressed in units of attomole ( $10^{-18}$  mol) of  $O_2$  consumed per second per cell  $[\text{amol}\cdot\text{s}^{-1}\cdot\text{ce}^{-1}]$ <sup>20</sup>,  
 239 numerically equivalent to  $[\text{pmol}\cdot\text{s}^{-1}\cdot(10^6\text{ ce})^{-1}]$ . At an  $O_2$  flow of  $100\text{ amol}\cdot\text{s}^{-1}\cdot\text{ce}^{-1}$  and a cell concentration  
 240 of  $10^9\text{ ce}\cdot\text{L}^{-1}$  ( $=10^6\text{ ce}\cdot\text{mL}^{-1}$ ),  $J_{V,O_2}$  is  $100\text{ nmol}\cdot\text{s}^{-1}\cdot\text{L}^{-1}$  ( $=100\text{ pmol}\cdot\text{s}^{-1}\cdot\text{mL}^{-1}$ ; Tab. 3b).

241

242 **Size-specific flux: per sample size.** Several sample types are not quantifiable numerically, *e.g.*, tissue  
 243 homogenate, in which case a sample-specific oxygen flow cannot be expressed discretely. Mass-specific  
 244 flux,  $J_{O_2/mX}$   $[\text{mol}\cdot\text{s}^{-1}\cdot\text{kg}^{-1}]$ , expresses respiration normalized per mass of the sample. Mass-specific oxygen  
 245 flux integrates the quality and density of mitochondria, and thus provides the appropriate normalization  
 246 for evaluation of tissue performance. When studying isolated mitochondria and homogenized or  
 247 permeabilized tissues and cells,  $J_{O_2/mX}$  should be independent of the mass-concentration of the subsample  
 248 obtained from the same tissue or cell culture.  $I_{O_2/Nce}$  can be directly compared only between cells of  
 249 identical size. To take into account differences in cell size, normalization is required to obtain cell size-  
 250 specific flux,  $J_{O_2/mce}$  or  $J_{O_2/Vce}$ <sup>21</sup> (Fig. 3).

251

252 **Marker-specific flux: per mitochondrial content.** To evaluate differences in mitochondrial respiration  
 253 independent of mitochondrial density, flux is normalized for structural or functional mt-elementary  
 254 markers, *mtE*, expressed in marker-specific mt-elementary units [mtEU] (Fig. 3). For example, citrate  
 255 synthase (CS) activity is a frequently applied functional *mtE* expressed in international units, IU  
 256  $[\mu\text{mol}\cdot\text{min}^{-1}]$  (1 IU of CS forms 1  $\mu\text{mol}$  of citrate per min; although the SI unit  $[\text{nmol}\cdot\text{s}^{-1}]$  would be  
 257 preferable). Then the mtEU is taken as  $[\mu\text{mol}\cdot\text{min}^{-1}]$  or  $[\text{nmol}\cdot\text{s}^{-1}]$ . Volume-specific oxygen flux,  $J_{V,O_2}$   
 258  $[\text{pmol}\cdot\text{s}^{-1}\cdot\text{mL}^{-1}]$ , is divided by CS activity expressed per chamber volume  $[\text{mtEU}\cdot\text{mL}^{-1}]$ , to obtain marker-  
 259 specific respiratory flux,  $J_{O_2/mtE}$   $[\text{pmol}\cdot\text{s}^{-1}\cdot\text{mtEU}^{-1}]$ . Alternatively,  $J_{O_2/mtE}$  is calculated from tissue mass-  
 260 specific flux of permeabilized muscle fibers,  $J_{O_2/m}$   $[\text{pmol}\text{ O}_2\cdot\text{s}^{-1}\cdot\text{mg}^{-1}]$ , divided by tissue mass-specific  
 261 CS activity  $[\text{mtEU}\cdot\text{mg}^{-1}]$ .  $J_{O_2/mtE}$  is independent of mitochondrial density. If the respirometric and  
 262 enzymatic assays are performed at an identical temperature, OXPHOS- or ET-capacity can be compared  
 263 with the capacity of CS as a regulatory enzyme in the tricarboxylic acid (TCA) cycle, which is of interest  
 264 in the context of metabolic flux control.

265 One cannot assume that quantitative changes in various markers — such as CS activity, other  
 266 mitochondrial enzyme activities or protein content — occur in parallel with one another<sup>22</sup>. It should be  
 267 established that the marker chosen is not selectively altered by the compared trait or treatment. In  
 268 conclusion, the normalization must reflect the question under investigation. On the other hand, the goal  
 269 of combining results across projects and institutions requires standardization of normalization for entry  
 270 into a databank.

271 Comparable to the concept of the respiratory acceptor control ratio,  $RCR = \text{State 3}/\text{State 4}$  (ref. <sup>9</sup>),  
 272 the most readily applied normalization is that of flux control ratios and flux control factors<sup>8,16</sup>. Then,  
 273 instead of a specific mt-enzyme activity, the respiratory activity in a reference state serves as the *mtE*,  
 274 yielding a dimensionless ratio of two fluxes measured consecutively in the same respirometric titration

275 protocol. Selection of the state of maximum flux in a protocol as the reference state — *e.g.*, ET-state in  
 276 *L/E* and *P/E* flux control ratios<sup>16</sup> — has the advantages of: (1) elimination of experimental variability in  
 277 additional measurements, such as determination of enzyme activity or tissue mass; (2) statistically  
 278 validated linearization of the response in the range of 0 to 1; and (3) consideration of maximum flux for  
 279 integrating a large number of metabolic steps in the OXPHOS- or ET-pathways. This reduces the risk  
 280 of selecting a functional marker that is specifically altered by the treatment or pathology, yet increases  
 281 the chance that the highly integrative pathway is affected, *e.g.*, the OXPHOS- rather than ET-pathway  
 282 in case of an enzymatic defect in the phosphorylation-pathway. In this case, additional information can  
 283 be obtained by reporting flux control ratios based on a reference state that indicates stable tissue mass-  
 284 specific flux.

## 286 Conclusions

287  
 288 Clarity of concepts on mitochondrial respiratory control can serve as a gateway to better diagnose  
 289 mitochondrial respiratory adaptations and defects linked to genetic variation, age-related health risks,  
 290 sex-specific mitochondrial performance, lifestyle with its effects on degenerative diseases, and thermal  
 291 and chemical environment. The challenges of measuring mitochondrial respiratory flux are matched by  
 292 those of normalization: We distinguish between (1) the instrumental *system* or *chamber* with volume *V*  
 293 and mass *m* defined by the system boundaries, and (2) the *sample* or *objects* with volume *V<sub>X</sub>* and mass  
 294 *m<sub>X</sub>* that are enclosed in the instrumental chamber. Metabolic O<sub>2</sub> flow per countable object increases as  
 295 the size of the object is increased. This confounding factor is eliminated by expressing respiration as  
 296 mass-specific or cell volume-specific O<sub>2</sub> flux. The present recommendations on coupling control states  
 297 and respiratory rates are focused on studies using mitochondrial preparations. Terms and symbols are  
 298 summarized in Tab. 4. These need to be complemented by considerations on pathway control of  
 299 mitochondrial respiration<sup>7,8,23</sup>, respiratory states and rates in living cells, respiratory flux control ratios,  
 300 and harmonization of experimental procedures. The present perspective is extended in a more detailed  
 301 overview on mitochondrial physiology<sup>24</sup>.

## 303 References

- 304 1. Cohen, E. R. et al. *IUPAC Green Book, 3rd Edition, 2nd Printing, IUPAC & RSC Publishing, Cambridge*  
 305 (2008).
- 306 2. Gnaiger, E. *Pure Appl Chem* **65**, 1983-2002 (1993).
- 307 3. Beard, D. A. *PLoS Comput Biol* **1**, e36 (2005).
- 308 4. Mitchell, P. *Nature* **191**, 144-148 (1961).
- 309 5. Mitchell, P. *Biochim Biophys Acta Bioenergetics* **1807**, 1507-1538 (2011).
- 310 6. Schmitt, S. et al. *Anal Biochem* **443**, 66-74 (2013).
- 311 7. Doerrier, C. et al. *Methods Mol Biol* **1782**, 31-70 (2018).
- 312 8. §Gnaiger, E. *Bioenerg Commun* **2020.2**, doi:10.26124/bec:2020-0002.v1 (2020).
- 313 9. Chance, B. & Williams, G. R. *J Biol Chem* **217**, 383-393 (1955).
- 314 10. Schneider, T. D. *IEEE Eng Med Biol Mag* **25**, 30-33 (2006).
- 315 11. Gnaiger, E. *Respir Physiol* **128**, 277-297 (2001).
- 316 12. Watt, I. N. et al. *Proc Natl Acad Sci U S A* **107**, 16823-16827 (2010).
- 317 13. Németh, B. et al. *FASEB J* **30**, 286-300 (2016).
- 318 14. Fell, D. *Understanding the control of metabolism. Portland Press* (1997).
- 319 15. Chance, B. & Williams, G. R. *J Biol Chem* **217**, 409-427 (1955).
- 320 16. Gnaiger, E. *Int J Biochem Cell Biol* **41**, 1837-1845 (2009).
- 321 17. Miller, G. A. *The science of words. Scientific American Library New York* (1991).
- 322 18. Forstner, H. & Gnaiger, E. In: *Polarographic Oxygen Sensors. Aquatic and Physiological Applications.*  
 323 *Gnaiger, E. & Forstner, H. (eds), Springer, Berlin, Heidelberg, New York*, 321-333 (1983).
- 324 19. Chance, B. & Williams, G. R. *Adv Enzymol Relat Subj Biochem* **17**, 65-134 (1956).
- 325 20. Wagner, B. A., Venkataraman, S. & Buettner, G. R. *Free Radic Biol Med* **51**, 700-712 (2011).
- 326 21. Renner, K. et al. *Biochim Biophys Acta* **1642**, 115-123 (2003).
- 327 22. Drahotka, Z. et al. *Physiol Res* **53**, 119-122 (2004).
- 328 23. Schöpf, B. et al. *Nat Commun* **11**, 1487 (2020).
- 329 24. §Gnaiger, E. et al. *Bioenerg Commun* **2020.1**, doi:10.26124/bec:2020-0001.v1 (2020).
- 330 25. Canton, M. et al. *Biochem J* **310**, 477-481 (1995).
- 331 26. Rich, P. R. *Encyclopedia Biol Chem* **1**, 467-472 (2013).
- 332

333 27. Lemieux, H., Blier, P. U. & Gnaiger, E. *Sci Rep* **7**, 2840 (2017).

334

335  To be released with DOI until acceptance by *Nat Metab*

336 *At present:*

337 8. Gnaiger, E. *Mitochondr Physiol Network 19.12. Oroboros MiPNet Publications, Innsbruck* (2014).

338 24. Gnaiger, E. et al. *MitoFit Preprint Arch* doi:10.26124/mitofit:190001.v6 (2019).

339

340 **\*Authors (MitoEAGLE Task Group):** Gnaiger Erich, Aasander Frostner Eleonor, Abdul Karim  
341 Norwahidah, Abdel-Rahman Engy Ali, Abumrad Nada A, Acuna-Castroviejo Dario, Adiele Reginald  
342 C, Ahn Bumsoo, Alencar Mayke Bezerra, Ali Sameh S, Almeida Angeles, Alton Lesley, Alves Marco  
343 G, Amati Francesca, Amoedo Nivea Dias, Amorim Ricardo, Anderson Ethan J, Andreadou Ioanna,  
344 Antunes Diana, Arago Marc, Aral Cenk, Arandarcikaite Odeta, Arias-Reyes Christian, Armand Anne-  
345 Sophie, Arnould Thierry, Avram Vlad F, Axelrod Christopher L, Bailey Damian M, Bairam Aida,  
346 Bajpeyi Sudip, Bajzikova Martina, Bakker Barbara M, Banni Aml, Bardal Tora, Barlow J, Bastos  
347 Sant'Anna Silva Ana Carolina, Batterson Philip M, Battino Maurizio, Bazil Jason N, Beard Daniel A,  
348 Bednarczyk Piotr, Beleza Jorge, Bello Fiona, Ben-Shachar Dorit, Bento Guida Jose Freitas, Bergdahl  
349 Andreas, Berge Rolf K, Bergmeister Lisa, Bernardi Paolo, Berridge Michael V, Bettinazzi Stefano,  
350 Bishop David J, Blier Pierre U, Blindheim Dan Filip, Boardman Neoma T, Boetker Hans Erik, Borchard  
351 Sabine, Boros Mihaly, Boersheim Elisabet, Borrás Consuelo, Borutaite Vilma, Botella Javier, Bouillaud  
352 Frederic, Bouitbir Jamal, Boushel Robert C, Bovard Josh, Bravo-Sagua Roberto, Breton Sophie, Brown  
353 David A, Brown Guy C, Brown Robert Andrew, Brozinick Joseph T, Buettner Garry R, Burtscher  
354 Johannes, Bustos Matilde, Calabria Elisa, Calbet Jose AL, Calzia Enrico, Cannon Daniel T, Cano  
355 Sanchez Maria Consolacion, Canto Alvarez Carles, Cardinale Daniele A, Cardoso Luiza HD, Carvalho  
356 Eugenia, Casado Pinna Marta, Cassar Samantha, Castelo Rueda Maria Paulina, Castilho Roger F,  
357 Cavalcanti-de-Albuquerque Joao Paulo, Cecatto Cristiane, Celen Murat C, Cervinkova Zuzana, Chabi  
358 Beatrice, Chakrabarti Lisa, Chakrabarti Sasanka, Chaurasia Bhagirath, Chen Quan, Chicco Adam J,  
359 Chinopoulos Christos, Chowdhury Subir Kumar, Cizmarova Beata, Clementi Emilio, Coen Paul M,  
360 Cohen Bruce H, Coker Robert H, Collin-Chenot Anne, Coughlan Melinda T, Coxito Pedro, Crisostomo  
361 Luis, Crispim Marcell, Crossland Hannah, Dahdah Norma Ramon, Dalgaard Louise T, Dambrova  
362 Maija, Danhelovska Tereza, Darveau Charles-A, Darwin Paula M, Das Anibh Martin, Dash Ranjan K,  
363 Davidova Eliska, Davis Michael S, Dayanidhi Sudarshan, De Bem Andreza Fabro, De Goede Paul, De  
364 Palma Clara, De Pinto Vito, Dela Flemming, Dembinska-Kiec Aldona, Detraux Damian, Devaux Yvan,  
365 Di Marcello Marco, Di Paola Floriana Jessica, Dias Candida, Dias Tania R, Diederich Marc, Distefano  
366 Giovanna, Djafarzadeh Siamak, Doermann Niklas, Doerrier Carolina, Dong Lan-Feng, Donnelly Chris,  
367 Drahota Zdenek, Duarte Filipe Valente, Dubouchaud Herve, Duchon Michael R, Dumas Jean-Francois,  
368 Durham William J, Dymkowska Dorota, Dyrstad Sissel E, Dyson Alex, Dzialowski Edward M, Eaton  
369 Simon, Ehinger Johannes K, Elmer Eskil, Endlicher Rene, Engin Ayse Basak, Escames Germaine,  
370 Evinova Andrea, Ezrova Zuzana, Falk Marni J, Fell David A, Ferdinandy Peter, Ferko Miroslav,  
371 Fernandez-Ortiz Marisol, Fernandez-Vizarra Erika, Ferreira Julio Cesar B, Ferreira Rita Maria P, Ferri  
372 Alessandra, Fessel Joshua Patrick, Festuccia William T, Filipovska Aleksandra, Fisar Zdenek, Fischer  
373 Christine, Fischer Michael J, Fisher Gordon, Fisher Joshua J, Fontanesi Flavia, Forbes-Hernandez  
374 Tamara Y, Ford Ellen, Fornaro Mara, Fuertes Agudo Marina, Fulton Montana, Galina Antonio, Galkin  
375 Alexander, Gallee Leon, Galli Gina L J, Gama Perez Pau, Gan Zhenji, Ganetzky Rebecca, Gao Yun,  
376 Garcia Geovana S, Garcia-Rivas Gerardo, Garcia-Roves Pablo Miguel, Garcia-Souza Luiz F, Garlid  
377 Keith D, Garrabou Gloria, Garten Antje, Gastaldelli Amalia, Gayen Jaur, Genders Amanda J, Genova  
378 Maria Luisa, Giampieri Francesca, Giovarelli Matteo, Glatz Jan FC, Goikoetxea Usandizaga Naroa,  
379 Goncalo Teixeira da Silva Rui, Goncalves Debora Farina, Gonzalez-Armenta Jenny L, Gonzalez-  
380 Franquesa Alba, Gonzalez-Freire Marta, Gonzalo Hugo, Goodpaster Bret H, Gorr Thomas A, Gourlay  
381 Campbell W, Grams Bente, Granata Cesare, Grefte Sander, Grilo Luis, Guarch Meritxell Espino,  
382 Gueguen Naig, Gumeni Sentiljana, Haas Clarissa, Haavik Jan, Hachmo Yafit, Haendeler Judith, Haider  
383 Markus, Hajrulahovic Anesa, Hamann Andrea, Han Jin, Han Woo Hyun, Hancock Chad R, Hand Steven  
384 C, Handl Jiri, Hansikova Hana, Hardee Justin P, Hargreaves Iain P, Harper Mary-Ellen, Harrison David  
385 K, Hassan Hazirah, Hatokova Zuzana, Hausenloy Derek J, Heales Simon JR, Hecker Matthias, Heiestad  
386 Christina, Hellgren Kim T, Henrique Alexandrino, Hepple Russell T, Hernansanz-Agustin Pablo,  
387 Hewakapuge Sudinna, Hickey Anthony J, Ho Dieu Hien, Hoehn Kyle L, Hoel Fredrik, Holland Olivia  
388 J, Holloway Graham P, Holzner Lorenz, Hoppel Charles L, Hoppel Florian, Hoppeler Hans, Houstek

389 Josef, Huete-Ortega Maria, Hyrossova Petra, Iglesias-Gonzalez Javier, Irving Brian A, Isola Raffaella,  
390 Iyer Shilpa, Jackson Christopher Benjamin, Jadiya Pooja, Jana Prado Fabian, Jandeleit-Dahm Karin,  
391 Jang David H, Jang Young Charles, Janowska Joanna, Jansen Kirsten M, Jansen-Duerr Pidder, Jansone  
392 Baiba, Jarmuszkiewicz Wieslawa, Jaskiewicz Anna, Jaspers Richard T, Jedlicka Jan, Jerome Estaquier,  
393 Jespersen Nichlas Riise, Jha Rajan Kumar, Jones John G, Joseph Vincent, Jurczak Michael J, Jurk  
394 Diana, Jusic Amela, Kaambre Tuuli, Kaczor Jan Jacek, Kainulainen Heikki, Kampa Rafal Pawel,  
395 Kandel Sunil Mani, Kane Daniel A, Kapferer Werner, Kapnick Senta, Kappler Lisa, Karabatsiakis  
396 Alexander, Karavaeva Iuliia, Karkucinska-Wieckowska Agnieszka, Kaur Sarbjot, Keijer Jaap, Keller  
397 Markus A, Keppner Gloria, Khamoui Andy V, Kidere Dita, Kilbaugh Todd, Kim Hyoung Kyu, Kim  
398 Julian KS, Kimoloi Sammy, Klepinin Aleksandr, Klepinina Lyudmila, Klingenspor Martin, Klocker  
399 Helmut, Kolassa Iris, Komlodi Timea, Koopman Werner JH, Kopitar-Jerala Natasa, Kowaltowski Alicia  
400 J, Kozlov Andrey V, Krajcova Adela, Krako Jakovljevic Nina, Kristal Bruce S, Krycer James R, Kuang  
401 Jujiao, Kucera Otto, Kuka Janis, Kwak Hyo Bum, Kwast Kurt E, Kwon Oh Sung, Laasmaa Martin,  
402 Labieniec-Watala Magdalena, Lagarrigue Sylviane, Lai Nicola, Lalic Nebojsa M, Land John M, Lane  
403 Nick, Laner Verena, Lanza Ian R, Laouafa Sofien, Laranjinha Joao, Larsen Steen, Larsen Terje S,  
404 Lavery Gareth G, Lazou Antigone, Ledo Ana Margarida, Lee Hong Kyu, Leeuwenburgh Christiaan,  
405 Lehti Maarit, Lemieux Helene, Lenaz Giorgio, Lerfall Joergen, Li Pingan Andy, Li Puma Lance, Liang  
406 Liping, Liepins Edgars, Lin Chien-Te, Liu Jiankang, Lopez Garcia Luis Carlos, Lucchinetti Eliana, Ma  
407 Tao, Macedo Maria Paula, Machado Ivo F, Maciej Sarah, MacMillan-Crow Lee Ann, Magalhaes Jose,  
408 Magri Andrea, Majtnerova Pavlina, Makarova Elina, Makrecka-Kuka Marina, Malik Afshan N,  
409 Marcouiller Francois, Markova Michaela, Markovic Ivanka, Martin Daniel S, Martins Ana Dias,  
410 Martins Joao D, Maseko Tumisang Edward, Maull Felicia, Mazat Jean-Pierre, McKenna Helen T,  
411 McKenzie Matthew, McMillan Duncan GG, Mendham Amy, Menze Michael A, Mercer John R, Merz  
412 Tamara, Messina Angela, Meszaros Andras, Methner Axel, Michalak Slawomir, Mila Guasch Maria,  
413 Minuzzi Luciele M, Moellering Douglas R, Moiso Nicoleta, Molina Anthony JA, Montaigne David,  
414 Moore Anthony L, Moore Christy, Moreau Kerrie, Moreira Bruno P, Moreno-Sanchez Rafael, Mracek  
415 Tomas, Muccini Anna Maria, Munro Daniel, Muntane Jordi, Muntean Danina M, Murray Andrew  
416 James, Musiol Eva, Nabben Miranda, Nair K Sreekumaran, Nehlin Jan O, Nemeč Michal, Nesci  
417 Salvatore, Neuffer P Darrell, Neuzil Jiri, Nevriere Remi, Newsom Sean A, Norman Jennifer, Nozickova  
418 Katerina, Nunes Sara, O'Brien Kristin, O'Brien Katie A, O'Gorman Donal, Olgar Yusuf, Oliveira Ben,  
419 Oliveira Jorge, Oliveira Marcus F, Oliveira Marcos Tulio, Oliveira Pedro Fontes, Oliveira Paulo J, Olsen  
420 Rolf Erik, Orynbayeva Zulfiya, Osiewacz Heinz D, Paez Hector, Pak Youngmi Kim, Pallotta Maria  
421 Luigia, Palmeira Carlos, Parajuli Nirmala, Passos Joao F, Passrigger Manuela, Patel Hemal H, Pavlova  
422 Nadia, Pavlovic Kasja, Pecina Petr, Pedersen Tina M, Perales Jose Carles, Pereira da Silva Grilo da  
423 Silva Filomena, Pereira Rita, Pereira Susana P, Perez Valencia Juan Alberto, Perks Kara L, Pesta  
424 Dominik, Petit Patrice X, Pettersen Nitschke Ina Katrine, Pichaud Nicolas, Pichler Irene, Piel Sarah,  
425 Pietka Terri A, Pinho Sonia A, Pino Maria F, Pirkmajer Sergej, Place Nicolas, Plangger Mario, Porter  
426 Craig, Porter Richard K, Pregoica Ines, Prigione Alessandro, Procaccio Vincent, Prochownik Edward  
427 V, Prola Alexandre, Pulinilkunnil Thomas, Puskarich Michael A, Puurand Marju, Radenkovic Filip,  
428 Ramzan Rabia, Rattan Suresh IS, Reano Simone, Reboredo-Rodriguez Patricia, Rees Bernard B,  
429 Renner-Sattler Kathrin, Rial Eduardo, Robinson Matthew M, Roden Michael, Rodrigues Ana Sofia,  
430 Rodriguez Enrique, Rodriguez-Enriquez Sara, Roesland Gro Vatne, Rohlena Jakub, Rolo Anabela  
431 Pinto, Ropelle Eduardo R, Roshanravan Baback, Rossignol Rodrigue, Rossiter Harry B, Rousar Tomas,  
432 Rubelj Ivica, Rybacka-Mossakowska Joanna, Saada Reisch Ann, Safaei Zahra, Salin Karine, Salvadego  
433 Desy, Sandi Carmen, Saner Nicholas, Santos Diana, Sanz Alberto, Sardao Vilma, Sarlak Saharnaz,  
434 Sazanov Leonid A, Scaife Paula, Scatena Roberto, Schartner Melanie, Scheibye-Knudsen Morten,  
435 Schilling Jan M, Schlattner Uwe, Schmitt Sabine, Schneider Gasser Edith Mariane, Schoenfeld Peter,  
436 Schots Pauke C, Schulz Rainer, Schwarzer Christoph, Scott Graham R, Selman Colin, Sendon Pamela  
437 Marie, Shabalina Irina G, Sharma Pushpa, Sharma Vipin, Shevchuk Igor, Shirazi Reza, Shiroma  
438 Jonathan G, Siewiera Karolina, Silber Ariel M, Silva Ana Maria, Sims Carrie A, Singer Dominique,  
439 Singh Brijesh Kumar, Skolik Robert A, Smenes Benedikte Therese, Smith James, Soares Felix  
440 Alexandre Antunes, Sobotka Ondrej, Sokolova Inna, Solesio Maria E, Soliz Jorge, Sommer Natascha,  
441 Sonkar Vijay K, Sova Marina, Sowton Alice P, Sparagna Genevieve C, Sparks Lauren M, Spinazzi  
442 Marco, Stankova Pavla, Starr Jonathan, Stary Creed, Stefan Eduard, Stelfa Gundega, Stepto Nigel K,  
443 Stevanovic Jelena, Stiban Johnny, Stier Antoine, Stocker Roland, Storder Julie, Sumbalova Zuzana,  
444 Suomalainen Anu, Suravajhala Prashanth, Svalbe Baiba, Swerdlow Russell H, Swiniuch Daria, Szabo



445 Ildiko, Szewczyk Adam, Szibor Marten, Tanaka Masashi, Tandler Bernard, Tarnopolsky Mark A,  
446 Tausan Daniel, Tavernarakis Nektarios, Teodoro Joao Soeiro, Tepp Kersti, Thakkar Himani, Thapa  
447 Maheshwor, Thyfault John P, Tomar Dhanendra, Ton Riccardo, Torp May-Kristin, Torres-Quesada  
448 Omar, Towheed Atif, Treberg Jason R, Tretter Laszlo, Trewin Adam J, Trifunovic Aleksandra, Trivigno  
449 Catherine, Tronstad Karl Johan, Trougakos Ioannis P, Truu Laura, Tuncay Erkan, Turan Belma, Tyrrell  
450 Daniel J, Urban Tomas, Urner Sofia, Valentine Joseph Marco, Van Bergen Nicole J, Van der Ende  
451 Miranda, Varricchio Frederick, Vaupel Peter, Vella Joanna, Vendelin Marko, Vercesi Anibal E,  
452 Verdaguer Ignasi Bofill, Vernerova Andrea, Victor Victor Manuel, Vieira Ligo Teixeira Camila,  
453 Vidimce Josif, Viel Christian, Vieyra Adalberto, Vilks Karlis, Villena Josep A, Vincent Vinnyfred,  
454 Vinogradov Andrey D, Viscomi Carlo, Vitorino Rui Miguel Pinheiro, Vlachaki Walker Julia, Vogt  
455 Sebastian, Volani Chiara, Volska Kristine, Votion Dominique-Marie, Vujacic-Mirski Ksenija, Wagner  
456 Brett A, Ward Marie Louise, Warnsmann Verena, Wasserman David H, Watala Cezary, Wei Yau-Huei,  
457 Weinberger Klaus M, Weissig Volkmar, White Sarah Haverty, Whitfield Jamie, Wickert Anika,  
458 Wieckowski Mariusz R, Wiesner Rudolf J, Williams Caroline M, Winwood-Smith Hugh, Wohlgemuth  
459 Stephanie E, Wohlwend Martin, Wolff Jonci Nikolai, Wrutniak-Cabello Chantal, Wuest Rob CI, Yokota  
460 Takashi, Zablocki Krzysztof, Zanon Alessandra, Zanou Nadege, Zaugg Kathrin, Zaugg Michael,  
461 Zdrzilova Lucie, Zhang Yong, Zhang Yizhu, Zikova Alena, Zischka Hans, Zorzano Antonio, Zujovic  
462 Tijana, Zvejniece Liga

Affiliations:

[https://www.bioenergetics-communications.org/index.php/BEC2020.1\\_doi10.26124bec2020-0001.v1](https://www.bioenergetics-communications.org/index.php/BEC2020.1_doi10.26124bec2020-0001.v1)

#### **Acknowledgements**

466 We thank Beno M for management assistance, and Rich PR for valuable discussions. This publication  
467 is based upon work from COST Action CA15203 MitoEAGLE, supported by COST (European  
468 Cooperation in Science and Technology), in cooperation with COST Actions CA16225 EU-  
469 CARDIOPROTECTION and CA17129 CardioRNA, and K-Regio project MitoFit funded by the  
470 Tyrolian Government.

#### **Author contributions**

474 This manuscript developed as an open invitation to scientists and students to join as coauthors in the  
475 bottom-up spirit of COST, based on a first draft written by the corresponding author, who integrated  
476 coauthor contributions in a sequence of Open Access versions. Coauthors contributed to the scope and  
477 quality of the manuscript, may have focused on a particular section, and are listed in alphabetical order.  
478 Coauthors confirm that they have read the final manuscript and agree to implement the  
479 recommendations into future manuscripts, presentations and teaching materials.

#### **Competing interests**

482 E.G. is founder and CEO of Oroboros Instruments, Innsbruck, Austria. The other authors declare no  
483 competing financial interests.

484

485 **Tables**

486

487

488

489

490

491

**Table 1 | Coupling control states and rates, and residual oxygen consumption in mitochondrial preparations.** Respiration- and phosphorylation-flux,  $J_{kO_2}$  and  $J_{P_{\gg}}$ , are rates, characteristic of a state in conjunction with the protonmotive force,  $pmF$ . Coupling states are established at kinetically-saturating concentrations of oxidizable 'fuel' substrates and  $O_2$ .

State	Rate	$J_{kO_2}$	$J_{P_{\gg}}$	$pmF$	Inducing factors	Limiting factors
LEAK	$L$	low, cation leak-dependent respiration	0	max.	back-flux of cations including proton leak, proton slip	$J_{P_{\gg}} = 0$ : (1) without ADP, $L(n)$ ; (2) max. ATP/ADP ratio, $L(T)$ ; or (3) inhibition of the phosphorylation-pathway, $L(O_{my})$
OXPHOS	$P$	high, ADP-stimulated respiration, OXPHOS-capacity	max.	high	kinetically-saturating [ADP] and $[P_i]$	$J_{P_{\gg}}$ by phosphorylation-pathway capacity; or $J_{kO_2}$ by ET-capacity
ET	$E$	max., noncoupled respiration, ET-capacity	0	low	optimal external uncoupler concentration for max. $J_{O_2,E}$	$J_{kO_2}$ by ET-capacity
ROX	$R_{ox}$	min., residual $O_2$ consumption	0	0	$J_{O_2,R_{ox}}$ in non-ET-pathway oxidation reactions	inhibition of all ET-pathways; or absence of fuel substrates

492

493  
494**Table 2 | Terms on respiratory coupling and uncoupling**

Term	$J_{kO_2}$	$P \gg O_2$	Notes	
intrinsic, no protonophore added	uncoupled	$L$	0	non-phosphorylating <b>LEAK-respiration</b> (Fig. 2)
	proton leak-uncoupled		0	component of $L$ , $H^+$ diffusion across the mtIM (Fig. 2b-d)
	inducibly uncoupled		0	by UCP1 or cation ( <i>e.g.</i> , $Ca^{2+}$ ) cycling; strongly stimulated by permeability transition (mtPT); experimentally induced by valinomycin in the presence of $K^+$
	decoupled		0	component of $L$ , proton slip when protons are effectively not pumped in the redox proton pumps CI, CIII and CIV or are not driving phosphorylation ( $F_1F_0$ -ATPase) <sup>25</sup> (Fig. 2b-d)
	loosely coupled		0	component of $L$ , lower coupling due to superoxide formation and bypass of proton pumps by electron leak with univalent reduction of $O_2$ to superoxide ( $O_2^{\cdot-}$ ; superoxide anion radical)
dyscoupled		0	mitochondrial dysfunction due to pathologically, toxicologically, environmentally increased uncoupling	
noncoupled	$E$		0	ET-capacity, non-phosphorylating respiration stimulated to maximum flux at optimum exogenous protonophore concentration (Fig. 2d)
well-coupled	$P$	high		<b>OXPHOS-capacity</b> , phosphorylating respiration with an intrinsic LEAK component (Fig. 2c)
fully coupled	$P - L$	max.		<b>OXPHOS-capacity</b> corrected for LEAK-respiration (Fig. 2a)
acoupled			0	electron transfer in mitochondrial fragments without vectorial proton translocation upon loss of vesicular (compartmental) integrity

495  
496

497 **Table 3 | Conversion of units**

498 **a. Conversion of O<sub>2</sub> flow,  $I_{O_2}$ , to SI units (International System of Units).**  
 499  $e^-$  is the number of electrons or reducing equivalents)

1 Unit		Multiplication factor	SI-unit
ng.atom O·s <sup>-1</sup>	(2 e <sup>-</sup> )	0.5	nmol O <sub>2</sub> ·s <sup>-1</sup>
ng.atom O·min <sup>-1</sup>	(2 e <sup>-</sup> )	8.333	pmol O <sub>2</sub> ·s <sup>-1</sup>
natom O·min <sup>-1</sup>	(2 e <sup>-</sup> )	8.333	pmol O <sub>2</sub> ·s <sup>-1</sup>
nmol O <sub>2</sub> ·min <sup>-1</sup>	(4 e <sup>-</sup> )	16.67	pmol O <sub>2</sub> ·s <sup>-1</sup>
nmol O <sub>2</sub> ·h <sup>-1</sup>	(4 e <sup>-</sup> )	0.2778	pmol O <sub>2</sub> ·s <sup>-1</sup>

500

501 **b. Conversion of units with preservation of numerical values**  
 502

Name	Frequently used unit	Equivalent unit	Notes
volume-specific flux, $J_{V,O_2}$	pmol·s <sup>-1</sup> ·mL <sup>-1</sup>	nmol·s <sup>-1</sup> ·L <sup>-1</sup>	1
	mmol·s <sup>-1</sup> ·L <sup>-1</sup>	mol·s <sup>-1</sup> ·m <sup>-3</sup>	
cell-specific flow, $I_{O_2/N_{ce}}$	pmol·s <sup>-1</sup> ·10 <sup>-6</sup> cells	amol·s <sup>-1</sup> ·cell <sup>-1</sup>	2
	pmol·s <sup>-1</sup> ·10 <sup>-9</sup> cells	zmol·s <sup>-1</sup> ·cell <sup>-1</sup>	3
cell number concentration, $C_{N_{ce}}$	10 <sup>6</sup> cells·mL <sup>-1</sup>	10 <sup>9</sup> cells·L <sup>-1</sup>	
mitochondrial protein concentration, $C_{mtE}$	0.1 mg·mL <sup>-1</sup>	0.1 g·L <sup>-1</sup>	
mass-specific flux, $J_{O_2/m}$	pmol·s <sup>-1</sup> ·mg <sup>-1</sup>	nmol·s <sup>-1</sup> ·g <sup>-1</sup>	4
volume, $V$	1,000 L	m <sup>3</sup> (1,000 kg)	
	L	dm <sup>3</sup> (kg)	
	mL	cm <sup>3</sup> (g)	
	μL	mm <sup>3</sup> (mg)	
	fL	μm <sup>3</sup> (pg)	
amount of substance concentration	M = mol·L <sup>-1</sup>	mol·dm <sup>-3</sup>	5

503 1 pmol: picomole = 10<sup>-12</sup> mol504 2 amol: attomole = 10<sup>-18</sup> mol505 3 zmol: zeptomole = 10<sup>-21</sup> mol

506

4 nmol: nanomole = 10<sup>-9</sup> mol5 fL: femtoliter = 10<sup>-15</sup> L

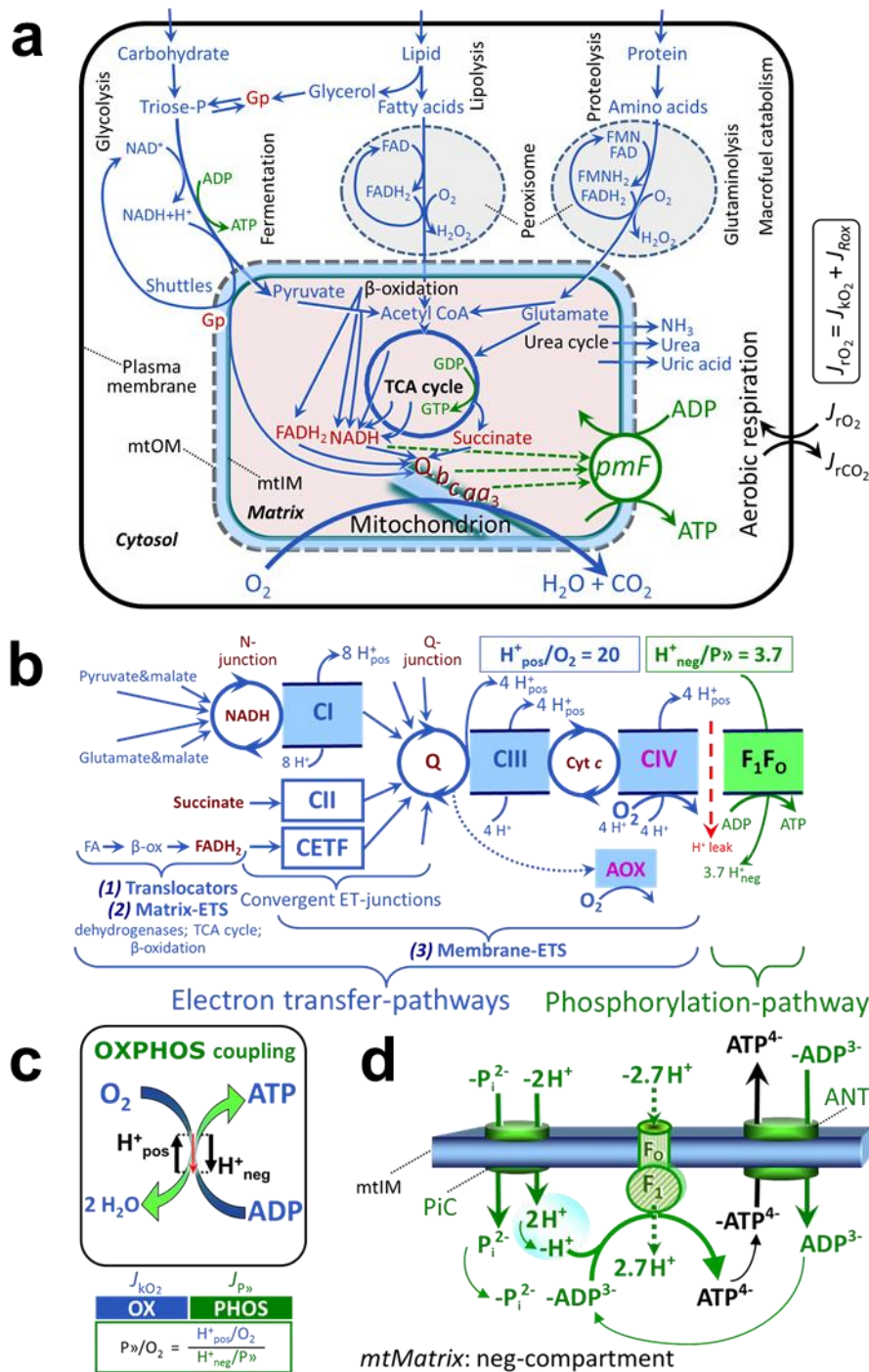
**Table 4 | Terms, symbols, and units.** SI base units are used, except for the liter [L = dm<sup>3</sup>]

Term	Symbol	Unit	Links and comments
adenosine diphosphate	ADP		Tab. 1; Fig. 1 and 2
adenosine triphosphate	ATP		Tab. 1; Fig. 1 and 2
ATP hydrolysis ATP→ADP	P«		Fig. 2b,c
catabolic reaction	k		Tab. 1 and 2; Fig. 1 and 2
catabolic respiration	$J_{kO_2}$	<i>varies</i>	Fig 1c, Fig. 2b-d
cell concentration (number [x])	$C_{N_{ce}}$	[x·L <sup>-1</sup> ]	for normalization of rate
coenzyme Q-junction	Q-junction		Fig. 1b
electron transfer Complexes	CI to CIV		Fig. 1b; F <sub>1</sub> F <sub>0</sub> -ATPase is not an ET- but a phosphorylation-pathway Complex, hence the term Complex V should not be used
electron transfer, state	ET		Tab. 1; Fig. 2a (State 3u)
electron transfer system	ETS		Fig. 1b
ET-capacity	$E$	<i>varies</i>	Tab. 1; Fig. 2a,d; rate
ET-excess capacity	$E-P$	<i>varies</i>	Fig. 2a
flow	$I$	[mol·s <sup>-1</sup> ]	Fig. 3; extensive quantity
flux	$J$	<i>varies</i>	Fig. 3; size-specific quantity
inorganic phosphate	P <sub>i</sub>		Fig. 1d
inorganic phosphate carrier	PiC		Fig. 1d
LEAK-state	<b>LEAK</b>		Tab. 1; Fig. 2a (compare State 4)
LEAK-respiration	$L$	<i>varies</i>	rate; Tab. 1; Fig. 2a,b
mass of sample or object $X$	$m_X$ or $m_{NX}$	[kg] or [kg·x <sup>-1</sup> ]	Fig. 3
mass, dry mass	$m_d$	[kg] or [kg·x <sup>-1</sup> ]	(dry weight)
mass, wet mass	$m_w$	[kg] or [kg·x <sup>-1</sup> ]	(wet weight)
mitochondria or mitochondrial	mt		compare mtDNA
mitochondrial elementary marker	$mtE$	[mtEU]	Fig. 3; quantity of mt-marker
mitochondrial elementary unit	mtEU	<i>varies</i>	Fig. 3; specific units for mt-marker
mitochondrial inner membrane	mtIM		Fig. 1 (MIM)
mitochondrial outer membrane	mtOM		Fig. 1 (MOM)
NADH-junction	N-junction		Fig. 1b
number concentration of $X$	$C_{NX}$	[x·L <sup>-1</sup> ]	for normalization of rate
number format	$\underline{N}$	[x]	Fig. 3
number of cells	$N_{ce}$	[x]	for normalization of rate
number of entities $X$	$N_X$	[x]	Fig. 3; for normalization of rate
O <sub>2</sub> concentration	$c_{O_2} = n_{O_2} \cdot V^{-1}$	[mol·L <sup>-1</sup> ]	[O <sub>2</sub> ]
O <sub>2</sub> flow per countable object	$I_{O_2/NX}$	[mol·s <sup>-1</sup> ·x <sup>-1</sup> ]	Fig. 3
O <sub>2</sub> flow per chamber	$I_{O_2}$	[mol·s <sup>-1</sup> ]	Fig. 3
O <sub>2</sub> flux, in reaction r	$J_{rO_2}$	<i>varies</i>	Fig. 1a
O <sub>2</sub> flux, volume-specific	$J_{V,O_2}$	[mol·s <sup>-1</sup> ·L <sup>-1</sup> ]	Fig. 3; per volume of chamber
O <sub>2</sub> flux, sample mass-specific	$J_{O_2/mX}$	[mol·s <sup>-1</sup> ·kg <sup>-1</sup> ]	Fig. 3; specify dry or wet mass
oxidative phosphorylation	OXPHOS		Fig. 1
OXPHOS-state	<b>OXPHOS</b>		Tab. 1; Fig. 2a; OXPHOS-state distinguished from the process OXPHOS (State 3 at kinetically-saturating [ADP] and [P <sub>i</sub> ])
OXPHOS-capacity	$P$	<i>varies</i>	rate; Tab. 1; Fig. 2a,c
permeability transition	mtPT		Tab. 2; MPT is widely used
phosphorylation flux ADP→ATP	$J_{P\gg}$	<i>varies</i>	Fig. 2b-d
phosphorylation of ADP to ATP	P»		Fig. 1
P»/O <sub>2</sub> ratio	P»/O <sub>2</sub>		mechanistic $Y_{P\gg/O_2}$ , calculated from pump stoichiometries; Fig. 1c

564	proton in the negative compartment	$H^+_{\text{neg}}$		Fig. 2b-d
565	proton in the positive compartment	$H^+_{\text{pos}}$		Fig. 1b,c; Fig. 2b-d
566	protonmotive flux to the negative			
567	compartment	$J_{\text{mH}^+\text{neg}}$	<i>varies</i>	Fig. 2d,f
568	protonmotive flux to the positive			
569	compartment	$J_{\text{mH}^+\text{pos}}$	<i>varies</i>	Fig. 2b,c,d
570	protonmotive force	$pmF$	[V]	Figures 1, 2A and 4; Table 1
571	rate of electron transfer in ET-state	$E$	<i>varies</i>	Tab. 1; ET-capacity
572	rate of LEAK-respiration	$L$	<i>varies</i>	Tab. 1; $L(n)$ , $L(T)$ , $L(O_{\text{my}})$
573	rate of oxidative phosphorylation	$P$	<i>varies</i>	Tab. 1; OXPHOS-capacity
574	rate of residual oxygen consumption	$Rox$	<i>varies</i>	Tab. 1
575	residual oxygen consumption, state	ROX		Tab. 1
576	sample type	$X$		
577	tricarboxylic acid cycle	TCA cycle		Fig. 1a
578	volume	$V$	[L]	volume of chamber
579	volume format	$\underline{V}$	[L]	Fig. 3
580	volume of sample or object $X$	$V_X$ or $V_{\underline{X}}$	[L] or $[L \cdot X^{-1}]$	Fig. 3
581	<hr/>			
582				

583 **Figures**

584



585

586

587

588

589

590

591

592

593

594

595

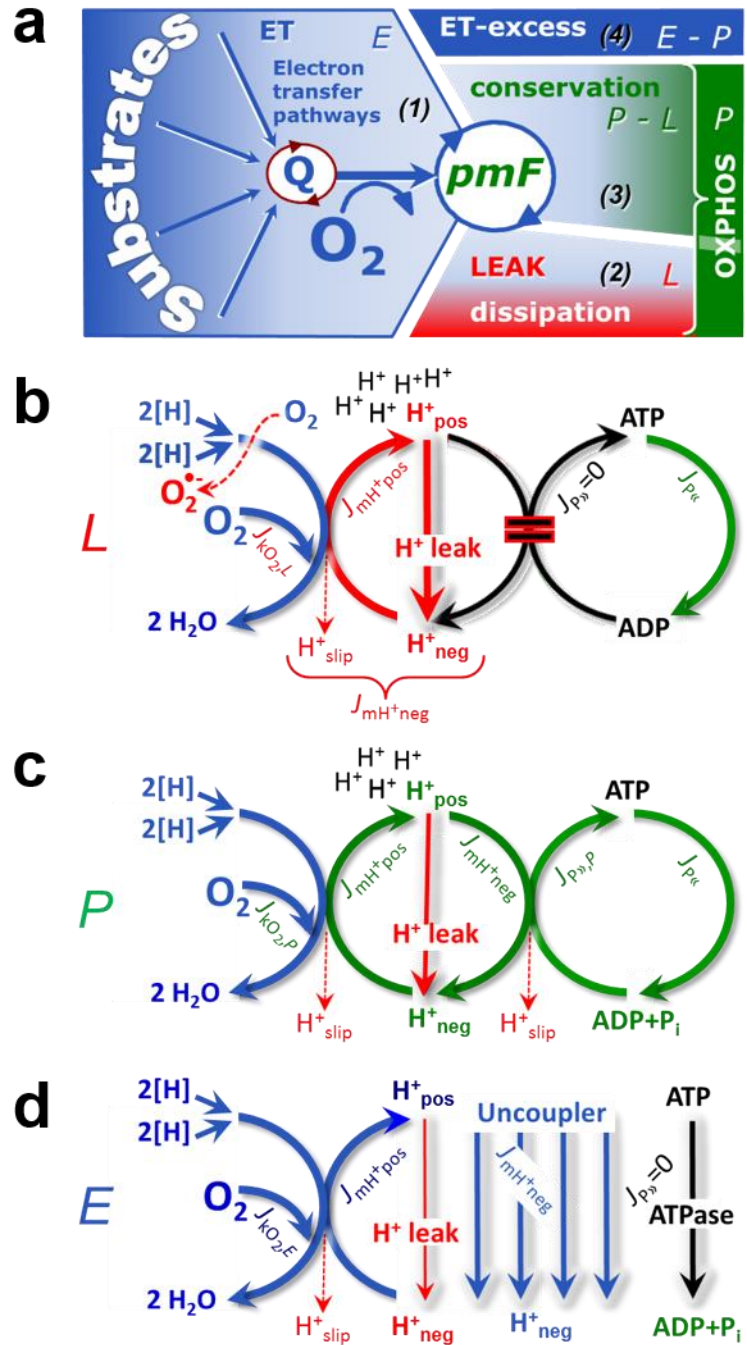
596

**Fig. 1. | Respiration and oxidative phosphorylation (OXPHOS).** (a) Cell respiration: uptake of small molecules and catabolism of macronutrients provide the mitochondrial fuel substrates (electron donors), which are oxidized with electron transfer to O<sub>2</sub> (electron acceptor). Dashed arrows indicate the connection between the redox proton pumps (respiratory Complexes CI, CIII and CIV) and the transmembrane protonmotive force, *pmF*. Coenzyme Q (Q) and the cytochromes *b*, *c*, and *aa<sub>3</sub>* are redox systems of the mitochondrial inner membrane, mtIM. Glycerol-3-phosphate, Gp. (b) Mitochondrial respiration: The mitochondrial electron transfer system (ETS) is (1) fueled by diffusion and transport of substrates across the mitochondrial outer and inner membranes (mtOM and mtIM), and in addition consists of the (2) matrix-ETS, and (3) membrane-ETS. Electron transfer converges from dehydrogenases at the NADH-junction (N-junction), and from CI,

597 CII and electron transferring flavoprotein complex (CETF) at the Coenzyme Q-junction  
598 (Q-junction). Unlabeled arrows converging at the Q-junction indicate additional ETS-  
599 sections with electron entry into Q through Gp-dehydrogenase, dihydroorotate  
600 dehydrogenase, proline dehydrogenase, choline dehydrogenase, and sulfide-ubiquinone  
601 oxidoreductase. The dotted arrow indicates the branched pathway of oxygen consumption  
602 by alternative quinol oxidase (AOX). ET-pathways are coupled to the phosphorylation-  
603 pathway. The  $H^+_{\text{pos}}/O_2$  ratio is the outward proton flux from the matrix space to the  
604 positively (pos) charged vesicular compartment, divided by catabolic  $O_2$  flux in the NADH-  
605 pathway<sup>26</sup>. The  $H^+_{\text{neg}}/P_{\gg}$  ratio is the inward proton flux from the inter-membrane space to  
606 the negatively (neg) charged matrix space, divided by phosphorylation flux of ADP to ATP.  
607 These stoichiometries are not fixed because of ion leaks and proton slip. Modified from  
608 ref. <sup>27</sup>. **(c) OXPHOS-coupling:** The  $H^+$  circuit couples  $O_2$  flux through the catabolic ET-  
609 pathway,  $J_{kO_2}$ , to flux through the phosphorylation-pathway of ADP to ATP,  $J_{P_{\gg}}$ . **(d)**  
610 Phosphorylation-pathway: the proton pump  $F_1F_0$ -ATPase (F-ATPase, ATP synthase),  
611 adenine nucleotide translocase (ANT), and inorganic phosphate carrier (PiC). The  $H^+_{\text{neg}}/P_{\gg}$   
612 stoichiometry is the sum of the coupling stoichiometry in the F-ATPase reaction ( $-2.7 H^+_{\text{pos}}$   
613 from the positive intermembrane space,  $2.7 H^+_{\text{neg}}$  to the matrix, *i.e.*, the negative  
614 compartment) and the proton balance in the translocation of  $ADP^{3-}$ ,  $ATP^{4-}$  and  $P_i^{2-}$  (negative  
615 for substrates) <sup>12</sup>. Modified from ref. <sup>8</sup>.  
616



617 **Fig. 2 | Respiratory states and**  
 618 **rates. (a)** Four-compartment model  
 619 of oxidative phosphorylation:  
 620 respiratory states (ET, OXPHOS,  
 621 LEAK) and corresponding rates ( $E$ ,  
 622  $P$ ,  $L$ ) are connected by the  
 623 protonmotive force,  $pmF$ . (1) ET-  
 624 capacity,  $E$ , is partitioned into (2)  
 625 dissipative LEAK-respiration,  $L$ ,  
 626 when the Gibbs energy change of  
 627 catabolic  $O_2$  flux is irreversibly lost,  
 628 (3) net OXPHOS-capacity,  $P-L$ , with  
 629 partial conservation of the capacity  
 630 to perform work, and (4) the ET-  
 631 excess capacity,  $E-P$ . (b) **LEAK-**  
 632 **rate,  $L$** : Oxidation only, since  
 633 phosphorylation is arrested,  $J_{P\gg} = 0$ ,  
 634 and catabolic  $O_2$  flux,  $J_{kO_2,L}$ , is  
 635 controlled mainly by the proton leak  
 636 and slip,  $J_{mH^{+neg}}$  (motive, subscript  
 637 m), at maximum protonmotive force.  
 638 ATP may be hydrolyzed by  
 639 ATPases,  $J_{P\ll}$ ; then phosphorylation  
 640 must be blocked. (c) **OXPHOS-**  
 641 **rate,  $P$** : Oxidation coupled to  
 642 phosphorylation,  $J_{P\gg}$ , which is  
 643 stimulated by kinetically-saturating  
 644 [ADP] and  $[P_i]$ , supported by a high  
 645 protonmotive force maintained by  
 646 pumping of protons to the positive  
 647 compartment,  $J_{mH^{+pos}}$ .  $O_2$  flux,  $J_{kO_2,P}$ ,  
 648 is well-coupled at a  $P\gg/O_2$  flux ratio  
 649 of  $J_{P\gg,P}/J_{O_2,P}$ . Extramitochondrial  
 650 ATPases may recycle ATP,  $J_{P\ll}$ . (d)  
 651 **ET- rate,  $E$** : Oxidation only, since  
 652 phosphorylation is zero,  $J_{P\gg} = 0$ , at  
 653 optimum exogenous uncoupler  
 654 concentration when noncoupled  
 655 respiration,  $J_{kO_2,E}$ , is maximum. The  
 656  $F_1F_0$ -ATPase may hydrolyze ATP  
 657 entering the mitochondria. Modified  
 658 from ref. <sup>8</sup>.  
 659



660 **Fig. 3 | Different meanings of**  
 661 **rate: flow and flux dependent on**  
 662 **normalization for sample or**  
 663 **instrumental chamber.**

664 Fundamental distinction between  
 665 metabolic rate related to the  
 666 experimental sample (left) or to  
 667 the instrumental chamber (right).  
 668 Left: Results are expressed as  
 669 mass-specific *flux*,  $J_{mX}$ , per mg  
 670 protein, dry or wet mass. Cell  
 671 volume,  $V_{ce}$ , may be used for  
 672 normalization (volume-specific  
 673 flux,  $J_{Vce}$ ). Normalization per  
 674 mitochondrial elementary marker,  
 675 *mtE*, relies on determination of mt-  
 676 markers expressed in various  
 677 mitochondrial elementary units [mtEU]. Right: Flow per instrumental chamber,  $I$ , or flux per chamber  
 678 volume,  $J_V$ , are reported for methodological reasons.  
 679

